

Appendix DR1. SEM, TEM and focused ion beam analytical methods, Figures DR1-DR3, and Table DR1

Precipitation of iron silicate nanoparticles in early Precambrian oceans marks Earth's first iron age

by Birger Rasmussen, Bryan Krapež, Janet R. Muhling and Alexandra A. Suvorova

ANALYTICAL METHODS

SEM analysis

Polished thin sections of BIF and chert were examined using backscattered-electron imaging (BSE) on *TESCAN VEGA 3* (LaB₆ source), *Zeiss 55 Supra* (field-emission source) and *FEI Verios* (field-emission source) scanning electron microscopes (SEM) located in the Centre for Microscopy, Characterisation and Analysis (CMCA) at the University of Western Australia (UWA). Each SEM was fitted with an *Oxford Instruments X-Max* energy dispersive X-ray detector (EDS) which was used for qualitative chemical analysis of mineral grains. Grains giving spectra with only O, Si and Fe peaks were interpreted to be greenalite, while spectra with minor peaks for Mg, Al and K, in addition to O, Si and Fe, were interpreted to be stilpnomelane.

Focused Ion Beam analysis

Foils for Transmission Electron Microscope (TEM) studies were cut from areas of chert with silicate nanoparticles located with BSE imaging in polished thin sections (Figure DR1). Focussed Ion Beam (FIB) techniques using an *FEI Helios NanoLab DualBeam* instrument located at Adelaide Microscopy, the University of Adelaide, were used to prepare the foils. Areas selected for analysis were first coated with a strip of Pt ~1 mm thick to protect the surface, then trenches ~5 mm deep were milled on either side of the strip using a Ga ion beam with 30 kV voltage and 21 nA current. The foil was then cut away from the sample and welded to a Cu TEM grid with a *Kleindiek nanotechnik* micromanipulator. The foils were thinned with the Ga ion beam at 30 kV and 0.28-0.92 nA, before cleaning at 5 kV and 47 pA, and polishing at 2 kV and 28 pA.

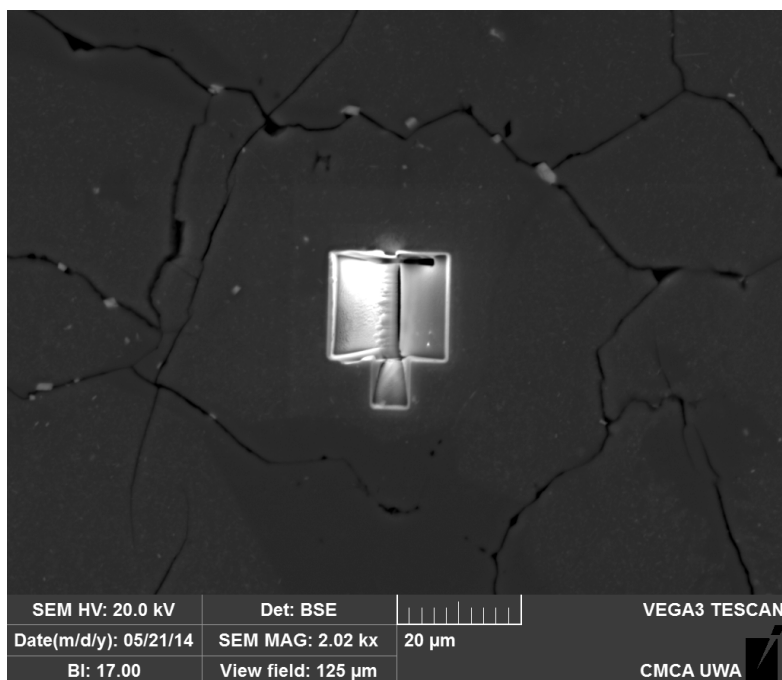


Figure DR1. Chert with polygonal fractures and dusted with nanoparticles, showing the location from which the TEM foil was removed by FIB milling. Drill-hole ABDP9, 288.23-288.36 m.

TEM analysis

Transmission electron microscope (TEM) data were obtained at 200 kV using an *FEI Titan G2 80–200* TEM/STEM with *ChemiSTEM* technology located at CMCA, UWA. High resolution TEM (HREM), high angle annular dark-field (HAADF STEM) images, and qualitative EDS maps were obtained to identify the Fe-rich silicate nanoparticles. HAADF images show two types of particles: lamellae of high brightness and lower brightness particles of more irregular shape (Figure DR2). EDS elemental maps for Fe and Si show that the brighter particles are Fe oxide (interpreted to be hematite) and that the other particles are Fe silicates (Figure DR2). The valence state of the Fe in the silicate particles has not been determined.

An HREM image of the Fe-rich silicate mineral from ABDP9 shows a series of parallel (001) lines with $\sim 7 \text{ \AA}$ interlayer spacing which is consistent with greenalite (Figure DR3). The d-spacings obtained from the Fourier Fast Transform (FFT) spot pattern show close matches to greenalite (see Table DR1). Some FFT patterns of the mineral show a set of satellite spots with diffuse intensities close to $hk0$ that is characteristic of greenalite (Figure 3) and indicates a regular modulation of the subcell structure. The satellite spacings, when present, consistently show a close fit to the spacings reported in Guggenheim et al. (1982) and Guggenheim et al. (1998) and indicate a subcell structure of 21 \AA . Similar TEM studies of a sample of BIF from drill-hole Silvergrass show that the Fe-silicate mineral in that sample is stilpnomelane.

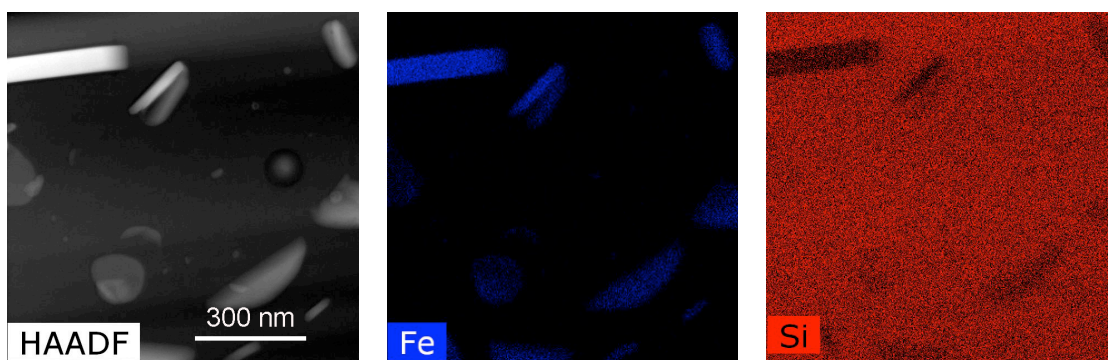


Figure DR2. HAADF STEM (Z-contrast) image (left) and ChemiSTEM elemental maps for Fe (centre) and Si (right). Drill-hole ABDP9, 288.23-288.36 m.

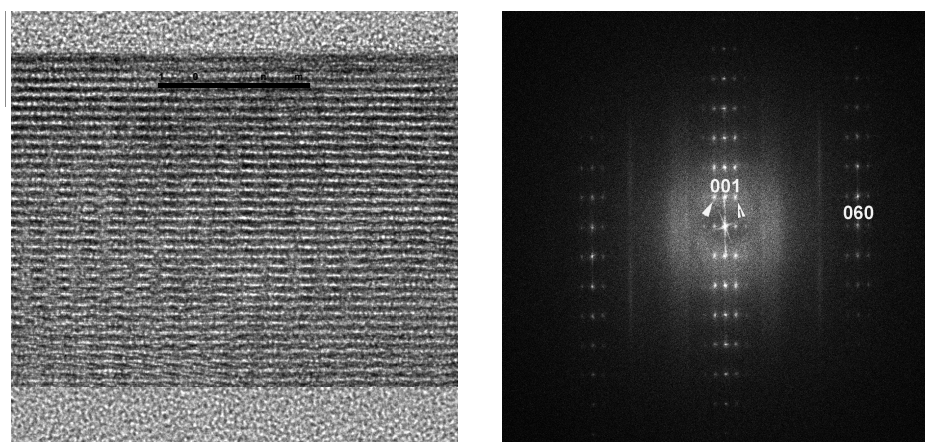


Figure DR3. HREM image of greenalite (left) and FFT pattern (right). The subcell reflections form $00l$ and $06l$ rows. The superlattice spacings are indicated by arrows.

Table DR1. Reported and measured d-spacings for greenalite

d (Å) calc. Guggenheim et al. (1982)	<i>hkl</i>	d (Å) and intensity http://www.mindat.org	d (Å) measured from HREM images
7.212	001	7.12 (80)	7.18
3.606	002	3.559 (80)	3.58
2.796	200	2.849(20)	
2.607	201,131	2.571 (100)	2.58
2.404	003		2.39
2.209	202, 132	2.184 (40)	
1.614	060,330	1.593 (60)	1.60
1.575	061,331	1.553 (40)	
1.442	005		1.43
1.203	006		1.19

REFERENCES CITED

- Guggenheim, S., Bailey, S.W., Eggleton, R.A., and Wilkes, P., 1982, Structural aspects of greenalite and related minerals: Canadian Mineralogist, v. 20, p. 1-18.
- Guggenheim, S., and Eggleton R.A., 1998, Modulated crystal structures of greenalite and caryopilite: a system with long-range, in-plane structural disorder in the tetrahedral sheet: Canadian Mineralogist, v. 36, p. 163-179.